A Technology-Agnostic MTJ SPICE Model with User-Defined Dimensions for STT-MRAM Scalability Studies

Jongyeon Kim[1], An Chen[2], Behtash Behin-Aein[2], Saurabh Kumar[1], Jian-Ping Wang[1], and Chris H. Kim[1]

[1]University of Minnesota, Minneapolis, MN 55455 USA
[2]GLOBALFOUNDRIES, Sunnyvale, CA 94085, USA

***Abstract*- The development of a scalable and user-friendly SPICE model is a key aspect of exploring the potential of spin-transfer torque MRAM (STT-MRAM). A self-contained magnetic tunnel junction (MTJ) SPICE model is proposed in this work which can reproduce realistic MTJ characteristics based on user-defined input parameters such as the free layer's length, width, and thickness. Using the propose model, scalability studies of both in-plane and perpendicular MTJs can be performed across different technology nodes with minimal effort, which differentiates this model from most previously reported models.**

I. Introduction

With complementary metal–oxide–semiconductor (CMOS) reaching its fundamental limits, the integration of spintronics into conventional CMOS is thoroughly being investigated to provide low static power as well as new functionalities while preserving the benefits of CMOS [1]. Spintronics applications such as MRAM or non-volatile flip-flops utilize a device structure called magnetic tunnel junction (MTJ) whose resistance states can be changed by spin-transfer torque (STT) current and read by sensing the tunneling magnetoresistance (TMR) difference. A key aspect of evaluating STT-MRAM technology is the development of a scalable MTJ compact model which can be used to incorporate realistic variability effects across different technology nodes.

Several SPICE compatible MTJ models have been reported in the past [2-4] to fulfil this goal. In [2], MTJ behaviors were emulated with SPICE subcircuits (e.g. bistable circuit, curve fitting circuit) based on empirical input parameters such as thermal stability (Δ), parallel and antiparallel resistance (R_P, R_{AP}), and the critical switching current (I_c). In order to capture realistic spin dynamics, the models in [3, 4] implemented the Landau-Lifshitz-Gilbert (LLG) equation using built-in SPICE elements such as resistors, capacitors, and voltage-/current-dependent voltage/current sources, considering physical parameters such as effective anisotropy field (H_{Keff}), MTJ dimensions, and material parameters. However, these models lack the flexibility for studying the scalability of various STT-MRAM designs since they still relied on a pre-calculated H_{Keff} value which is a function of the MTJ width, length, and thickness dimensions.

For a compact model to be useful in evaluating STT-MRAM circuits across different technologies, it has to be scalable for future nodes and at the same time be fully-compatible with SPICE. To satisfy these requirements, we propose a scalable physics-based SPICE MTJ model with user-defined dimensional and material parameters. The main improvements of this work compared to previous SPICE MTJ models are summarized as follows.

- We provide a self-contained MTJ model that comprehends anisotropy, STT switching, TMR, and temperature effect, which is reconfigurable using user-defined input parameters.
- Our model generates H_{Keff} for all types of anisotropy sources such as shape, crystal, and interface, which makes it possible to simulate both in-plane and perpendicular MTJs in *any* given technology node.
- Spin dynamics computed by incorporating the dimension-dependent H_{Keff} into the LLG equation, instantly reflects dimensional changes in the MTJ performance, which enables more accurate scalability and variability analyses.
- The stochastic nature of the magnetization switching is captured by changing the initial magnetization angle. The switching distribution can be easily obtained using this simple approach.
- The temperature dependency of various material parameters is included considering internal Joule heating during the switching process.

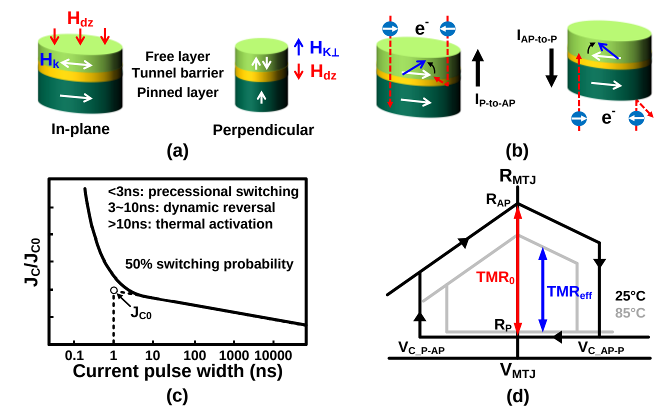

Fig. 1. Basic MTJ characteristics (a) In-plane and perpendicular magnetic anisotropy. (b) Bi-directional STT switching. (c) Critical switching current as a function of pulse width. (d) Temperature-dependent R-V hysteresis curve.

II. MTJ Physics To Be Modeled

A. Magnetic Anisotropy

Several MTJ options exist depending on the physical origin of magnetic anisotropy (MA): namely, shape anisotropy-based in-plane MTJ (IMTJ), crystal anisotropy-based perpendicular MTJ (c-PMTJ), and interface anisotropy-based perpendicular MTJ (i-PMTJ).

For IMTJ, the origin of shape anisotropy is the demagnetizing field (H_d) which is stronger along the axis with a shorter dimension. As a result, the magnetization (M) has a tendency to align with the longest axis giving rise to shape-dependent magnetic anisotropy. The free layer of the IMTJ can be regarded as an elongated thin film with the shortest axis being in the z-direction. Here, M stays in the x-y plane as shown in Fig. 1 (a). The shape anisotropy field ($H_{K,shape}$) can be expressed as:

$$H_{K,shape} = 4\pi(N_{dx} - N_{dy})M_s. \tag{1}$$

where M_s is the saturation magnetization and N_d is the geometry-dependent demagnetizing factor. However, the IMTJ has to overcome a large H_{dz} resulting in a large switching current.

PMTJ on the other hand can provide a lower switching current compared to IMTJ since H_{dz} assists the magnetization switching by partially canceling out the perpendicular anisotropy field ($H_{K\perp}$) as shown in Fig. 1(a). However, in order to maintain the proper orientation of the M, $H_{K\perp}$ must overpower H_{dz}. This can be achieved by using either a high crystal anisotropy (K_u) using $L1_0$-phase alloys (e.g. CoPt, FePd) or interface anisotropy (K_i) using a CoFeB layer thinner than its critical thickness (t_c). The effective perpendicular anisotropy field ($H_{K\perp eff}$) is given by:

$$H_{K\perp eff} = H_{K\perp} - H_{dz} = 2K_{\perp}/M_s - 4\pi N_{dz} M_s. \quad (2)$$

For c-PMTJ, $K_{\perp}$ is equivalent to K_u of the specific material. For i-PMTJ, $K_{\perp}$ is replaced with K_i/t_F ($=2\pi M_s^2 t_c/t_F$) where t_F is the free layer thickness.

B. STT Switching

Bi-directional spin-polarized electrons exert spin torque to the free layer and induce magnetization switching in the desired direction as shown in Fig 1(b). If we treat the free layer as a single magnetic domain, the spin dynamics can be characterized with a time-varying unit magnetization vector given as $\bar{M}(t)=[M_x(t), M_y(t), M_z(t)]$. When a switching current density (J) is applied to the MTJ, the spin-polarized current exerts spin torque to flip $\bar{M}$ against H_{Keff}. Here, the spin direction of polarized current depends on the magnetization of the pinned layer $\bar{M}_p$. Since H_{Keff} of an IMTJ is mainly governed by H_d, its magnetization vector can be denoted as follows:

$$\bar{H}_{K=eff}(t) = -4\pi M_s [N_{dx} M_x(t), N_{dy} M_y(t), N_{dz} M_z(t)]. \quad (3)$$

On the other hand, H_{Keff} of a PMTJ is the combination of $H_{K\perp}$ and H_d so its vector notation is given by

$$\bar{H}_{K\perp eff}(t) = [0,0,(\frac{2K_{\perp}}{M_S})M_z(t)] - 4\pi M_s [N_{dx} M_x(t), N_{dy} M_y(t), N_{dz} M_z(t)]. \quad (4)$$

The dynamics of $\bar{M}(t)$ is generally described by the LLG equation with H_{Keff} incorporated as follows:

$$\frac{1+\alpha^2}{\gamma}\cdot\frac{d\bar{M}}{dt} = -\bar{M}\times\bar{H}_{Keff} - \alpha\cdot\bar{M}\times(\bar{M}\times\bar{H}_{Keff}) + \frac{\hbar PJ}{2et_F M_s}\cdot\bar{M}\times(\bar{M}\times\bar{M}_p). \quad (5)$$

where γ is the gyromagnetic ratio, α is the damping constant, $\hbar$ is the reduced Planck's constant, P is the spin polarization factor, and e is the electron charge. When the switching current exceeds the critical value, the dynamic precession motion overcomes H_{Keff} and flips the magnetization to the opposite stable state.

C. Temperature Effect

The transient behavior of an MTJ is non-deterministic due to the random thermal field which causes the magnetization vector to deviate from the easy axis by an angle determined by the MTJ temperature. Moreover, at long current pulses (i.e. >10ns), an increase in internal temperature due to Joule heating excites the thermal field thereby reducing the switching current as shown in Fig. 1(c). For fast precessional switching, which is more relevant in today's high speed STT-MRAM, the stochastic behavior can be captured using a switching probability (P_{sw}) as a function of the critical initial angle (θ_c), which can be described as:

$$P_{sw} = 1 - \int_0^{\theta_c} \frac{\sin\theta\exp(-\Delta\sin^2\theta)}{\int_0^{\frac{\pi}{2}}\sin\theta\exp(-\Delta\sin^2\theta)d\theta}d\theta,\ \Delta = \frac{E_b}{k_B T}. \quad (6)$$

Where T is the temperature, E_b is the energy barrier, k_B is the Boltzmann constant. Material parameters related to device performance also have a temperature dependency as follows:

$$M_s(T) = M_{s0}(1 - T/T_c)^{\beta}. \quad (7)$$

$$P(T) = P_0(1 - \alpha_{sp} T^{3/2}). \quad (8)$$

where M_{s0} and P_0 are the saturation magnetization and the polarization factor at absolute zero temperature, T_c is the Curie temperature, β and α_{sp} are the material-dependent constants.

D. TMR

An MTJ can be considered as a voltage-controlled variable resistance represented by the resistance-voltage (R-V) hysteresis curve shown in Fig. 1(d). The resistance ratio at a zero bias (TMR_0) is defined as (R_{AP}-R_P)/R_P. Since the TMR depends on temperature and bias voltage, TMR_{eff} is a better measure to evaluate read/write performances. The voltage and temperature dependency of TMR can be captured using the temperature-dependent polarization equation:

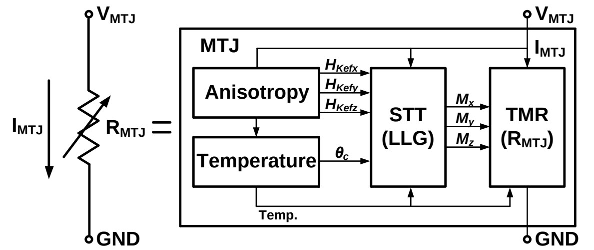

Fig. 2. Simulation framework of the proposed MTJ model.

Input	Description	Remark
W	Free layer width	Δ dependent
L	Free layer length	Δ dependent
t_F	Free layer thickness	Δ dependent
α	Magnetic damping factor	Material related
M_{s0}	Saturation magnetization, 0K	Material related
P_0	Polarization factor, 0K	Material related
K_u	Crystal anisotropy constant	for c-PMTJ
t_c	Critical thickness	for i-PMTJ
T_0	Initial temperature	Ambient
P_{sw}	Switching probability	by initial angle
RA	Resistance-area product	Measured data
asym	Bidirectional I_c asymmetry	Measured data
MA	In-plane/Perpendicular selection	0/1
State	Parallel/Anti-parallel selection	0/1

Fig. 3. User-defined input parameters of the proposed MTJ model.

$$TMR(T,V) = \frac{2P_0^2(1-\alpha_{sp}T^{3/2})^2}{1-P_0^2(1-\alpha_{sp}T^{3/2})^2}\cdot\frac{1}{1+(V/V_0)^2}. \quad (9)$$

Here, V_0 is a fitting parameter. Once RA value is determined, R_P and R_{AP} can be calculated by considering MTJ area and TMR.

III. MODEL FRAMEWORK AND IMPLEMENTATION

The physical behaviors of a real MTJ were recreated using four dedicated SPICE subcircuits: namely, anisotropy, STT, TMR, and temperature subcircuits as shown in Fig. 2. Once the type of MTJ is selected, the anisotropy circuit generates H_{Keff} as derived in (3) and (4) for the given MTJ dimensions and material parameters. Meanwhile, the temperature circuit estimates θ_c at a given temperature as well as the switching probability given in (6), which sets the initial position of $\bar{M}$. When a bias voltage (V_{MTJ}) is applied to the MTJ, a charge current (I_{MTJ}) passes through the MTJ. The I_{MTJ} fed to the STT circuit generates a spin-polarized current and triggers dynamic spin motion returning x, y, and z coordinates of the time-

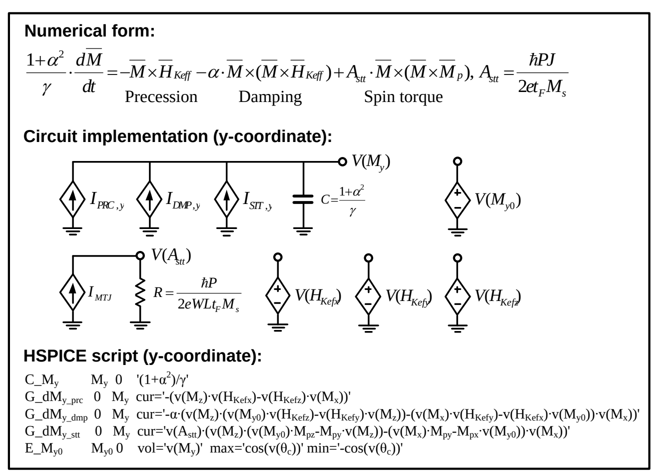

Fig. 4. SPICE implementation of LLG equation (only y-coordinate shown here for simplicity).

varying vector $\bar{M}$. The Cartesian coordinates are converted to spherical coordinates by the TMR circuit generating a relative angle between the free and pinned layers to determine the MTJ resistance (R_{MTJ}). The I_{MTJ} is also an input to the temperature circuit to estimate the increase in internal temperature due to Joule heating. The updated temperature is fed back to the STT and TMR circuits modifying material parameters that have a temperature dependency as given in (7) and (8). Fig. 3 shows input knobs which provide sufficient flexibility to explore various aspects of MTJ switching behavior.

For full compatibility with SPICE, each subcircuit was implemented using basic circuit elements such as resistors, capacitors, and voltage-/current-dependent voltage/current sources. For example, the constants and variables included in the physical equations were defined using SPICE parameters (i.e. .PARAM command) and voltage-dependent voltage sources, respectively. Multiplication between a coefficient and a variable was implemented using a resistor (V=I·R). In this way, all the internal values are represented using node voltages. The most critical part of the model implementation is the dynamic spin motion described by the LLG equation, which is presented in Fig. 4. Numerically, the LLG equation is a differential equation containing cross products of three dimensional vectors (i.e. $\bar{M}$, $\bar{M}_p$, and $\bar{H}_{Keff}$). In terms of circuit implementation, the differential behavior of $\bar{M}$ can be captured using a capacitor with voltage-dependent current sources connected in parallel, which emulates an incremental charge build-up over time in the capacitor: $I=C{\cdot}dV/dt$. Three current sources represent the precession, damping, and spin torque terms in the LLG equation, and their vector cross product can be rewritten into linear forms as described in the SPICE script. M_{y0} is the additional node to set the initial angle in case of consecutive switching. To solve a three-dimensional LLG equation, separate circuits for x, y, and z coordinates are implemented in the same way. The anisotropy and TMR circuits are simply implemented with SPICE parameters and voltage sources, while the temperature circuit uses a distributed RC line model which emulates the heat diffusion equation as suggested in [4].

IV. Model Verification

In order to verify the accuracy of the model, simulation results were compared with experiment data. In Fig. 5, the simulated dynamic spin motions of IMTJ and PMTJ are presented alongside the temperature dependency of several material parameters. The results show a clear contrast between the magnetization trajectories of IMTJ and PMTJ, which was not observed using the previous models [2-4]. In Fig. 6(a), simulation results show good agreement with the 50% switching probability contour where switching time was measured as a function of bias voltage [5]. The model can be extended to track a higher percentile contour such as 99.99%. In Fig. 6(b), the simulated R-V hysteresis curves reproduce the MTJ resistance and the critical switching voltage (V_c) at different temperatures [6]. The flexibility of

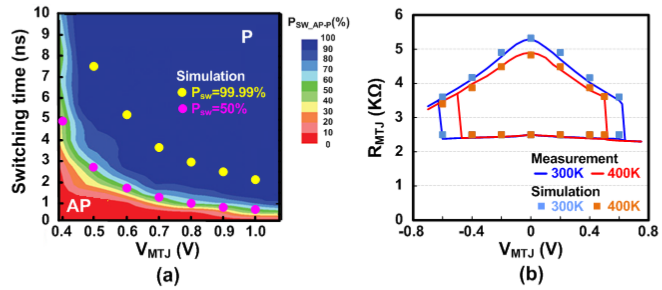

Fig. 6. Simulation results compared to experimental data. (a) Switching time as a function of bias voltage across the MTJ. (b) Temperature-dependent R-V hysteresis curve.

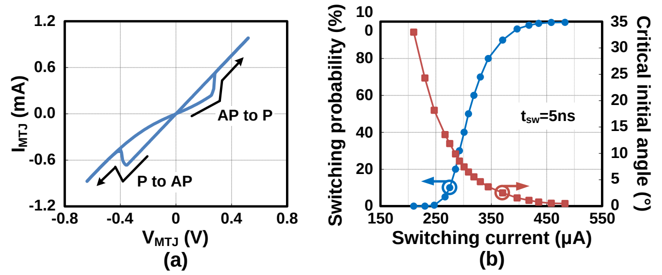

Fig. 7. MTJ switching behavior characterization. (a) I-V hysteresis curve with asymmetric V_c for bi-directional switching. (b) Switching probability as a function of switching current using an initial angle dependency.

our model makes it easy to incorporate additional MTJ characteristics. For instance, asymmetry in the I-V hysteresis curve shown in Fig. 7(a) can be included using a user-defined asymmetry factor. Fig. 7(b) shows the switching probability according to the critical initial angle, providing detailed info regarding the switching current requirement.

V. Model Application

A. Scalability Studies of In-Plane and Perpendicular MTJs

As mentioned earlier, H_{Keff} in our model is calculated using the x, y, and z dimensions of an MTJ and therefore the model can be used for studying the detailed scaling behavior of different MTJs (i.e. IMTJ, c-PMTJ, and i-PMTJ). Fig. 8 shows an example of such a study for a 128 MB cache memory with a 10 year retention failure probability target of 0.01%. The thermal stability Δ required for this target retention time can be met by adjusting the MTJ dimensions in different ways depending on the anisotropy source. For instance, a higher Δ can be obtained for IMTJ by either increasing the aspect ratio (AR) or increasing t_F while ensuring single domain switching (e.g. AR<3). For c-PMTJ, K_u is increased to $2.0{\times}10^6$J/m^3 (FePdX based free layer) while maintaining t_F of 0.45nm to induce high H_{dz} for low I_c. Below a 20nm MTJ width, it is necessary to increase the t_F. For i-PMTJ, t_F must be reduced in order to increase K_i which in turn

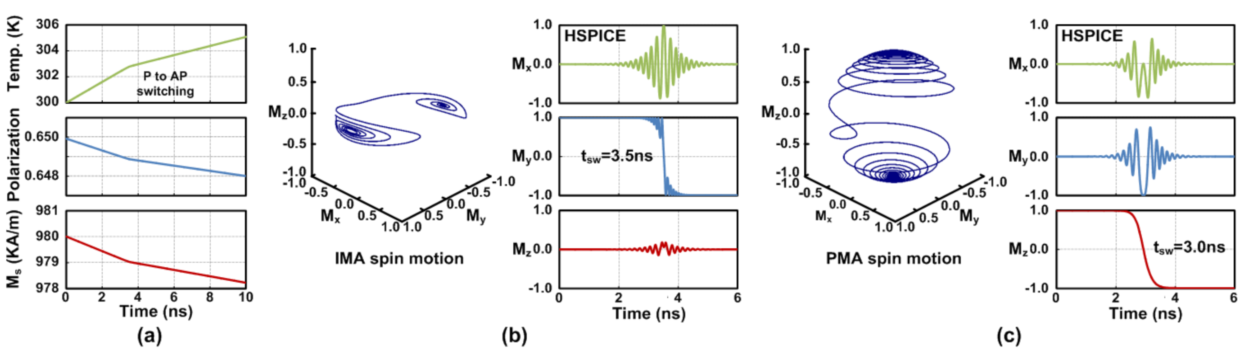

Fig. 5. MTJ switching dynamics verification. (a) Temperature dependency of material parameters during a switching event. (b) Dynamic spin motion for in-plane MTJ. (c) Dynamic spin motion for perpendicular MTJ.

MTJ width (nm)			60	50	40	30	20
IMTJ (CoFeB)	M_s=1077, P=0.6	AR	2.35	2.65	3	3	3
		t_F (nm)	2.00	2.00	2.10	2.58	3.50
		α	0.007	0.007	0.0068	0.006	0.0055
		Remark	AR ↑		t_F ↑ , t_F dependent α		
c-PMTJ (FePdX)	M_s=1077, P=0.51, α=0.03	K_u	0.92	1.01	1.18	1.55	2.00
		t_F (nm)	0.45	0.45	0.45	0.45	0.65
		Remark	constant t_F, K_u ↑				t_F ↑
i-PMTJ (CoFeB)	Ms=1077, P=0.6, t_c=1.5nm	t_F (nm)	1.47	1.42	1.32	2.99	2.31
		α	0.013	0.015	0.018	0.006	0.0062
		Remark	t_F ↓, t_F dependent α			Dual interface	

*Δ=70 (85°C), M_s (10^3A/m), K_u (10^6J/m^3)

Fig. 8. Scaling scenario example for IMTJ, c-PMTJ, and i-PMTJ under iso-retention (10 years under a 0.01% retention failure criteria).

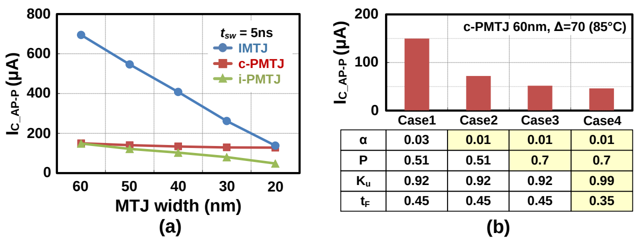

	Case1	Case2	Case3	Case4
α	0.03	0.01	0.01	0.01
P	0.51	0.51	0.7	0.7
K_u	0.92	0.92	0.92	0.99
t_F	0.45	0.45	0.45	0.35

Fig. 9. Scaling analysis of in-plane and perpendicular MTJs. (a) Scalability of I_c under iso-retention and iso-switching delay (t_{sw}=5ns). (b) Sensitivity analysis of I_c under different material assumptions for c-PMTJ.

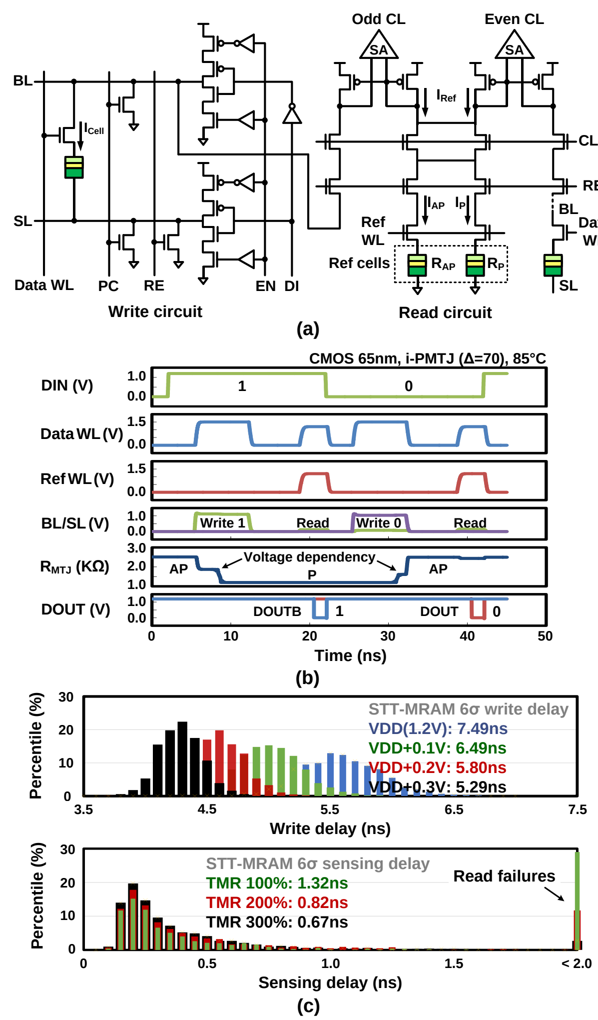

Fig. 10. STT-MRAM statistical simulation results. (a) Schematic for read/write circuitry. (b) Waveforms for STT-MRAM read/write operation. (c) Write and sensing delay distributions under process variation (10^3 MC runs).

increases the Δ. Below a 30nm MTJ width, a double interface i-PMTJ may have to be introduced to meet Δ. Thickness dependency of α in CoFeB is also considered for both IMTJ and i-PMTJ. Based on this scenario, i-PMTJ shows the smallest I_c at a 20nm MTJ width as shown in Fig. 9(a). While IMTJ shows a rapid reduction in I_c with scaling, c-PMTJ shows a relatively constant I_c indicating its I_c scaling is more sensitive to material parameters rather than dimensional parameters as shown in Fig. 9(b).

B. Variability Studies of STT-MRAM Read and Write Delays

The proposed model was also used to study the statistical behavior of STT-MRAM read and write delays considering geometrical variation in both MTJ and CMOS. Fig. 10(a) shows the simplified read/write circuit schematic used for this experiment. MTJs were assumed to be connected in the reverse direction (i.e. so called top-pinned MTJ structure) to balance bi-directional switching. Bi-directional write current drivers and dual-voltage WL drivers are used to ensure sufficient write margin. Self-referencing MTJ cells and a mid-point reference circuit generating $I_{Ref}=(I_{AP}+I_P)/2$ are incorporated for good readability. As shown in Fig. 10(b), the STT-MRAM critical path comprising of the MTJ and CMOS shows good read/write operations. Using this simulation setup, realistic variation is introduced to MTJ input parameters (i.e. W, L, t_F, RA) as well as CMOS input parameters (i.e. transistor W, L, V_{th}, T_{ox}). Fig. 10(c) shows write and sensing delay distributions with 6σ values denoted in the figure legends. The write delay is measured from WL activation to the time when the $\bar{M}$ flips whereas the sensing delay is measured from WL activation to the point when the bitline voltage difference reaches 25mV. As the write voltage increases, the switching delay distribution becomes narrower due to the faster precession at the higher bias voltage. For the sensing delay, the mismatch of read current paths between data and reference cells directly affects sensing voltages so a higher TMR is required for better read margin.

VI. Conclusion

In this work, we proposed a physics-based MTJ model with dimension-dependent H_{Keff} specifically designed for evaluating the scalability and variability of STT-MRAM circuits. The compact model was validated with measured data and has shown to successfully reproduce realistic MTJ characteristics in SPICE. Using the proposed model, we benchmarked the scalability of various MTJ technologies under iso-retention condition and simulated read and write delay variations. The proposed compact model will be useful for evaluating current and future STT-MRAM technology options, providing specific guidelines to the spintronics device and circuits community. The MTJ compact model along with documentation will shortly be available on a public download website.

Acknowledgment

This work was supported in part by C-SPIN, one of six centers of STARnet, a Semiconductor Research Corporation program, sponsored by MARCO and DARPA.

References

[1] S. A. Wolf, et al. "The promise of nanomagnetics and spintronics for future logic and universal memory," Proc. IEEE, 2010.

[2] J. D. Harms, et al. "SPICE macromodel of spin-torque-transfer-operated magnetic tunnel junctions," TED, 2010.

[3] Z. Xu, et al. "Compact Modeling of STT-MTJ for SPICE Simulation," ESSDERC, 2013.

[4] G. D. Panagopoulos, et al. "Physics-based SPICE-compatible compact model for simulating hybrid MTJ/CMOS circuits," TED, 2013.

[5] H. Zhao, et al. "Low writing energy and sub nanosecond spin torque transfer switching of in-plane magnetic tunnel junction for spin torque transfer random access memory," JAP, 2011.

[6] C. Lin, et al. "45nm low power CMOS logic compatible embedded STT MRAM utilizing a reverse-connection 1T/1MTJ cell," IEDM, 2009.